Title
Drug Delivery Nanoparticles with Locally Tunable Toxicity Made Entirely from a Light-Activatable Prodrug of Doxorubicin

Journal
Pharmaceutical Research, 34(10)

ISSN
0724-8741

Authors
Schutt, Carolyn
Ibsen, Stuart
Zahavy, Eran
et al.

Publication Date
2017-10-01

DOI
10.1007/s11095-017-2205-4

Peer reviewed

HHS Public Access

Author manuscript

Pharm Res. Author manuscript; available in PMC 2019 October 05.

Published in final edited form as:

Pharm Res. 2017 October ; 34(10): 2025–2035. doi:10.1007/s11095-017-2205-4.

Drug Delivery Nanoparticles with Locally Tunable Toxicity Made Entirely from a Light-Activatable Prodrug of Doxorubicin

Carolyn Schutt[1,*], **Stuart Ibsen**[2], **Eran Zahavy**[3], **Santosh Aryal**[4], **Stacey Kuo**[5], **Selin Esener**[5], **Michael Berns**[1], **Sadik Esener**[5]

[1]Department of Bioengineering, University of California San Diego, 9500 Gilman Dr. MC 0412, La Jolla, California 92093-0412, USA

[2]Moores Cancer Center, University of California San Diego, La Jolla, CA 92093, USA

[3]Department Biochemistry and Molecular Genetics, Israel Institute for Biological Research, P.O. Box 19, Ness-Ziona 74100, Israel

[4]Department of Chemistry, Nanotechnology Innovation Center of Kansas State, Kansas State University, Manhattan, KS 66506, USA

[5]Department of Nanoengineering, University of California San Diego, La Jolla, CA 92093 USA

Abstract

Purpose: A major challenge facing nanoparticle-based delivery of chemotherapy agents is the natural and unavoidable accumulation of these particles in healthy tissue resulting in local toxicity and dose-limiting side effects. To address this issue, we have designed and characterized a new prodrug nanoparticle with controllable toxicity allowing a locally-delivered light trigger to convert the payload of the particle from a low to a high toxicity state.

Methods: The nanoparticles are created entirely from light-activatable prodrug molecules using a nanoprecipitation process. The prodrug is a conjugate of doxorubicin and photocleavable biotin (DOX-PCB).

Results: These DOX-PCB nanoparticles are 30 times less toxic to cells than doxorubicin, but can be activated to release pure therapeutic doxorubicin when exposed to 365 nm light. These nanoparticles have an average diameter of around 100 nm and achieve the maximum possible prodrug loading capacity since no support structure or coating is required to prevent loss of prodrug from the nanoparticle.

Conclusions: These light activatable nanoparticles demonstrate tunable toxicity and can be used to facilitate future therapy development whereby light delivered specifically to the tumor tissue would locally convert the nanoparticles to doxorubicin while leaving nanoparticles accumulated in healthy tissue in the less toxic prodrug form.

Keywords

Light-activatable; prodrug; doxorubicin; nanoparticle drug delivery vehicle; DNA intercalation

[*]Corresponding Author carolyn.schutt@gmail.com.

1. Introduction

The size range that allows nanoparticle-based drug delivery vehicles to achieve long circulation times *in-vivo* also allows them to passively extravasate through discontinuous endothelium, like that found in tumors.(1) This is a significant advantage in the case of chemotherapy delivery because the particles will preferentially accumulate in tumor tissue while passing through healthy tissue with continuous endothelium, such as sensitive heart tissue. (2–4)

However, one of the main challenges is that discontinuous endothelium is not limited only to the tumor tissue. Other healthy tissue also allows for extravasation and can locally accumulate circulating particles to toxic levels. Such healthy tissues include the creases of the skin on the hands and feet where it is thought that constant motion causes natural microdamage to the blood vessels allowing nanoparticles to extravasate(5) causing dose-limiting side effects.(6) Particles in this size range can also be actively taken up by healthy cells in the reticulo-endothelial system (RES).(7) Polyethylene glycol (PEG) surface coatings can delay accumulation, especially in the RES, but over time the particles still accumulate in healthy tissue including the liver.(8) There is no particle size range that will allow for long circulation times while avoiding extravasation and accumulation in these healthy tissues.(9, 10)

In this work we address the issue of unavoidable accumulation in healthy tissue by designing a nanoparticle (NP) drug delivery vehicle that is comprised entirely of a light-activatable prodrug. This prodrug shows significantly reduced toxicity compared to the pure drug but can be activated to its therapeutic form by light exposure. The ability to control or tune the toxicity of the drug delivery nanoparticles through light exposure after they have been injected into the body could allow for two spatially separate populations of nanoparticles to be created. The first would be the nanoparticles that unintentionally accumulate in healthy tissue including the liver, which would not be exposed to light and thus would remain in the low toxicity state. The second would be the particles that accumulate in the target tumor tissue which can then be preferentially triggered to a highly toxic state by light exposure (Figure 1).

The prodrug used to make the nanoparticles was developed using the chemotherapy drug doxorubicin (DOX). It consisted of a photocleavable linker(11) (PCB) covalently bound to DOX to create the prodrug DOX-PCB. This rendered the DOX less toxic to tissue with the unique ability to restore full therapeutic function when photo-triggered.(12) The photoactivation mechanism has been fully described and the release of intact doxorubicin confirmed by HPLC/mass spectrometry and ^{1}H NMR analysis.(12) Active DOX was shown to be released *in-vivo* from free DOX-PCB prodrug molecules inside tumors when the activating light was delivered to the center of the tumor using a fiber optic coupled light emitting diode setup.(13)

The choice of the prodrug trigger that restores the prodrug to its therapeutic form is critical to assure tumor specificity. The use of light is distinct from traditional activation mechanisms that rely on the biochemistry of the tumor. These biochemical triggers include

differences in the microenvironment between the tumor and the normal tissue such as tumor-associated hypoxia or low pH(14, 15), as well as enzymatic cleavage by enzymes which the tumor over-expresses.(16–18) The main challenge is that these biochemical triggers are often present in both tumor and non-tumor tissue(19, 20), especially in the liver where there is both a high level of enzymatic activity and a high level of particle accumulation. The light-based trigger can achieve a higher level of specificity than biochemical triggers because the activating wavelength of light can be delivered specifically to the tumor tissue using light emitting diode (LED) and fiber optic technology. Recent developments in LED manufacturing enable elements to be made with sub-millimeter dimensions(21) which could allow them to be inserted(13) or implanted anywhere a biopsy needle, endoscope, or catheter can go.

The photocleavable linker in DOX-PCB has been shown to be resistant to metabolic degradation(12) which prevents undesired activation of the prodrug in healthy tissue regions, including the liver(12, 22), but is activated by exposure to 365 nm light. This wavelength showed low absorption by internal tissue(23) including DNA(24) reducing the possibility of bioeffects. The 365 nm light is highly absorbed by melanin(25) which makes the delivered light the only significant source of this wavelength inside the body. This prevents external sources of 365 nm light from causing uncontrolled release within the body. Previous studies have shown that 365 nm light delivered by a fiber optic to the center of a 1 cm diameter tumor is heavily scattered by the tissue.(13) This scattering exposes the entire tumor volume to the 365 nm light at a sufficient intensity to cause activation of DOX-PCB in therapeutic amounts from the tumor center to the tumor margins.(13)

The light-activatable prodrug would benefit from a nanoparticle carrier by increasing circulation time and tumor accumulation in a similar way that DOX benefits from Doxil®, an FDA-approved nanoliposomal formulation of DOX.(1, 26) The 80–120 nm size(10) and PEG surface coatings of Doxil® particles change the pharmacokinetics and biodistribution(27) of DOX in humans leading to an increase in circulation half-life from 9 hours for the free DOX to 42 hours with Doxil®.(10) The Doxil® particle also leads to increased DOX concentrations within tumors(10) and reduced concentrations within heart tissue.(2–4)

However, the active DOX payload of Doxil® causes skin ulcerations and irritation (Palmar-plantar erythrodysesthesia) when the particles unintentionally accumulate in the hands and feet which is a major dose-limiting side effect.(6) Doxil® will also accumulate in the bone marrow(7, 28) both via the reticulo-endothelial system(7) and by extravasation(9) due to the bone marrow’s discontinuous endothelium(29) leading to dose-limiting myelosuppression.(6) This unintentional accumulation of nanoparticles in healthy tissue remains a major concern.

The major breakthrough in this new light-activatable nanoparticle design, when compared to Doxil®, is that any prodrug which accumulates in healthy tissue will remain in the low-toxicity state. Only the prodrug delivered to the tumor tissue will receive the activating light exposure converting it to toxic DOX. The light activation mechanism of our new prodrug

nanoparticles can potentially create higher doses of active drug in the correct tissue location while causing minimal toxicity to healthy tissues.

2. Methods and Materials

2.1 Materials

Doxorubicin hydrochloride (DOX) was purchased from Qventas (Branford, CT) and Sigma (St. Louis, MO). Water soluble photocleavable biotin–NHS (PCB) was purchased from Ambergen (Watertown, MA). High pressure liquid chromatography (HPLC) grade acetonitrile was purchased from Fisher Scientific (Fairlawn, NJ). The human lung cancer cell line A549 and the PTK2 (*Potorous tridactylus*) kidney epithelial cell line (ATCC CCL-56) were purchased from the American Type Culture Collection (Manassas, VA). Trypsin-EDTA (ethylenediaminetetraacetic acid) used for cell culture was purchased from Mediatech, Inc. (Manassas, VA). All DMEM (Dulbecco's Modified Eagle Medium) media and the penicillin-streptomycin used as a media supplement were purchased from Gibco (Invitrogen, Grand Island, NY). Fetal bovine serum (FBS) used as a media supplement was purchased from Hyclone Laboratories Inc. (Logan, UT). Dulbecco's phosphate buffered saline (DPBS) was also purchased from Hyclone Laboratories Inc. (Logan, UT). All water was purified using the Milli-Q purification system from Millipore Corporation (Billerica, MA). XTT was purchased from Sigma (St. Louis, MO).

2.2 DOX-PCB Nanoparticle Synthesis

The DOX-PCB prodrug was synthesized using the procedure described in Ibsen et al. (12). To form nanoparticles from the DOX-PCB prodrug, a single-step nanoprecipitation method was used. The DOX-PCB prodrug was first dissolved in acetonitrile at a concentration of 0.1 mg/ml. A 168 μl volume of this solution was aspirated into a 1 ml syringe fitted with a 30 gauge 1 inch needle, and then added dropwise to 2 ml of ultrapure water under vortex. The hydrophobic ends of the prodrug molecules clustered together to form particles in order to minimize contact with the water. The resulting sample was stirred gently for 48 hours at room temperature while open to the atmosphere to evaporate the acetonitrile. This evaporation was performed to help ensure the stability of the nanoparticles and the biocompatibility of the sample. The sample was protected from ambient light during the stirring process.

The particles were then concentrated using a centrifugal evaporator to remove the desired amount of water. The particles did not aggregate as they were concentrated under the centrifugal force. Care was taken to ensure the evaporation rate did not result in the freezing of the water. DOX-PCB concentration was measured through light absorption using a Nanodrop ND-1000 spectrophotometer (Thermo Fisher Scientific, Waltham, MA). All DOX-PCB nanoparticle solution concentrations are given in terms of DOX-PCB molecule content.

2.3 Particle Characterization

The DOX-PCB nanoparticles were characterized using several different methods. The size distribution of the particles was first evaluated by the Nanoparticle Tracking Analysis (NTA)

technique using a NanoSight LM10 system (NanoSight Ltd., Amesbury, UK) at room temperature. Two samples of 300 μl volume were introduced into the viewing unit for the particles to be tracked and sized on a particle-by-particle basis using the NTA technique. Size is reported as the average of the peak value of the size distribution from each sample. A video clip of the particles' Brownian motion was also acquired using the NanoSight system.

The size results acquired by NTA were confirmed using a Zetasizer Nano-ZS dynamic light scattering (DLS) system (Malvern Instruments, Worcestershire, UK) at room temperature with backscattering angle of 173°. Size measurements were obtained in triplicate along with polydispersity indices. Zeta potential measurements were also acquired in triplicate using this instrument.

The morphology of the nanoparticles was characterized using scanning electron microscopy (SEM) with a Phillips XL30 SEM system. The manufactured nanoparticle sample was diluted 10,000 times from its original concentration to allow observation of individual particles. A 2 μl volume of the diluted sample was placed on the surface of a polished silicon wafer and allowed to dry at room temperature overnight. The sample was coated with chromium and then imaged.

2.4 Particle Surface Characterization

The presence of the biotin-terminated PEG tail on the surface of the nanoparticles was investigated using a binding assay with streptavidin-coated Sepharose microbeads and uncoated Sepharose beads as a control. To replace the beads' 20% ethanol storage solutions with water, samples of 50 μl of Streptavidin Sepharose High Performance beads (GE Healthcare Life Sciences, Little Chalfont, UK) and uncoated Sepharose control beads (Sepharose CL-4B, GE Healthcare Life Sciences, Little Chalfont, UK) were each diluted by adding 1 ml Milli-Q water, then spun down with subsequent removal of 1 ml supernatant, followed by the addition of 50 μl fresh Milli-Q water. From these resulting bead samples, 15 μl of each bead type was added to 30 μl of unconcentrated DOX-PCB NP, and the solutions were mixed by pipette aspiration and incubated for 10 minutes. Brightfield and fluorescent images of the streptavidin-coated and uncoated beads with DOX-PCB NP were then taken using a Nikon E600 upright fluorescence microscope with a 20x objective.

2.5 Light-Activated Drug Release Characterization

The nanoparticle samples were evaluated for their release of pure DOX after receiving various amounts of 365 nm light exposure. Samples of 10 μl of DOX-PCB nanoparticles at 31 μM were placed into individual wells in a 96-well flat bottom assay plate (BD Biosciences, San Jose, CA) with opaque black walls and a clear bottom. The black walls helped to prevent reflections of 365 nm light inside the well and ensure uniformity of exposure between samples. The clear lid of the plate was fitted on top to help reduce the evaporation rate of the water. The samples were exposed to 2.3 mW/cm^2 of light from a Mercury Short Arc HBO bulb from OSRAM (München, Germany) with a 330–380 nm bandpass filter for increasing durations of time from 0 to 60 min. This measured light intensity took into account the absorption of 365 nm light by the lid. The samples were then collected and their volumes adjusted with water to 10 μl if any evaporation occurred.

In an in-vivo application, the DOX that was released from the nanoparticles would immediately diffuse away from the particle and associate with plasma proteins, cellular proteins, and DNA. In the specific case of this experiment the DOX-PCB nanoparticles were suspended at a high concentration in pure water which could allow the free DOX released from the particles to immediately associate with other particles. To help prevent free DOX from being sequestered into other particles, the 365 nm light exposed samples were then mixed with dimethyl sulfoxide (DMSO) in a 0.2/1 v/v ratio. The samples were then bath sonicated for 5 min. The presence of DMSO in the sample helped to keep the released DOX in solution so that it could be quantified by LC-MS/MS.

The DOX content of the samples was then quantified by LC-MS/MS using an Agilent 1260 liquid chromatography (LC) system coupled with a Thermo LCQdeca mass spectrometer (MS). The LC-MS/MS analysis used positive ion mode electrospray ionization (ESI) as the ion source with source voltage of 5 kV, capillary temperature of 250°C, auxiliary gas flow rate of 20 units, and sheath gas flow rate of 80 units. A CAPCELL MG III C-18 column (Catalog number 92744, ID 2.0 mm × length 50 mm, particle size 3 μm) was used (with guard column) for LC separation. The mobile phase A was 5% methanol in water with 0.1% formic acid. The mobile phase B was pure methanol with 0.1% formic acid. The LC gradient was increased from 30% mobile phase B to 95% mobile phase B in a duration of 10 minutes, then held at 95% B for 5 minutes, brought back to 30% B in 1 minute, and then held at 30% B for 6 minutes. The LC flow rate was held at 0.20 ml/min. Using these LC conditions, the DOX and the two isomers of DOX-PCB were separately eluted from the LC column with a retention time of about 9.8 minutes for DOX, and about 13.2 and 13.7 minutes for the two isomers of DOX-PCB. DOX had a molecular ion peak at m/z 544 ($[M+H]^+$). Under positive ion mode ESI-MS/MS analysis, a major fragment peak of DOX was seen at m/z 396.8 with a normalized collision energy of 30%. Both of the DOX-PCB isomers had molecular ion peaks at m/z 1244.4 ($[M+Na]^+$). Under positive ion mode, the ESI-MS/MS analysis showed a major fragment peak ($[M+Na]^+$) at m/z 848.3 with a normalized collision energy of 35%. Selected reaction monitoring (SRM) mode was used to acquire the m/z 396.8 fragment ion peak which was used for quantification of the DOX. The statistical analysis was performed using MATLAB R2015a software.

2.6 Cellular Localization

The intracellular localization of the DOX-PCB nanoparticles and pure DOX was studied using the PTK2 (*Potorous tridactylus*) kidney epithelial cell line (ATCC CCL-56). These cells were used because they are susceptible to DOX and remain flat during mitosis, allowing for enhanced visualization of the nuclear region. This visualization capability was important since one of the main therapeutic modes of action for DOX is through DNA intercalation. The DOX-PCB nanoparticles and pure DOX are both naturally fluorescent which allowed these agents to be easily tracked through the cell. The PTK2 cells were grown in high glucose DMEM with 4.5 g/L glucose, 10% FBS, sodium pyruvate, L-Glutamine, and penicillin-streptomycin. The cells were plated in glass bottom petri dishes (MatTek Corporation, Ashland, MA) and allowed to adhere to the bottom surface.

A 1 ml media solution of DOX-PCB nanoparticles was prepared by first adding 10x DPBS to a 4.1 μM solution of DOX-PCB nanoparticles in water to achieve a 1x DPBS concentration, and then adding the resulting solution to the same DMEM media described above to achieve a final DOX-PCB content of 2 μM. This spiked media sample was then added to the PTK2 cells seeded in the glass bottom petri dishes after removing their previous growth media. A 1 ml media solution of 2 μM DOX was prepared in the same manner with the DPBS content matched to the above nanoparticle solution, and the DOX media solution was added to the cells in the same manner as described above. The cells were incubated with the spiked media samples for 2 hours. Live fluorescent images of the cells were obtained using a Zeiss Axiovert 200 M Microscope (Zeiss, Thornwood, NY) using a 63x phase III, NA 1.4 oil immersion objective. All microscope control and imaging utilized the RoboLase system (32).

To study the change in cellular localization after activation, the cells incubated with the DOX-PCB nanoparticles were exposed to the 365 nm light source for 120 seconds. The cells were then allowed to incubate in the 365 nm light-exposed media for 1 hour. The cells were reanalyzed using the microscopy system described above. The RoboLase system allowed the same cells that where imaged before 365 nm light exposure to be relocated and imaged again after 365 nm light exposure.

2.7 Cytotoxicity

An IC_{50} study was conducted to determine the toxicity of the DOX-PCB nanoparticles to cancer cells before and after 365 nm light exposure relative to free DOX using the human lung cancer cell line A549. The cells were grown on sodium pyruvate-free DMEM media containing L-glutamine, 4.5 g/L of glucose, penicillin-streptomycin and 10% Fetal Bovine Serum. The adherent cells in the expansion flask were detached using trypsin (.25% trypsin / 2.21 mM EDTA) and plated onto a 96-well plate at a density of 10^4 cells per well in 100 μL of media. The cells were incubated at 37°C overnight to allow them to adhere to the bottom of the well.

Experiments were run in two replicates under three different conditions. The first condition was incubation with pure DOX, the second was incubation with DOX-PCB nanoparticles with no 365 nm light exposure, and the third was incubation with DOX-PCB nanoparticles that had previously been exposed to 60 min of 365 nm light (2.3 mW/cm^2) from the same light source used in the light-activated drug release characterization study. The 365 nm light exposure itself has been shown to have no significant effect on cell viability with 60 min of exposure (12).

The spiked media samples were prepared ahead of time using stock solutions of 200 μM DOX and 200 μM DOX-PCB nanoparticles in water. A sample of the pure DMEM media described above was concentrated to 80% of the original volume. The concentrated media was rediluted to its original volume using the stock solutions of drug to achieve solutions of DOX and DOX-PCB nanoparticles at 13.3 μM in the media. A 1/3 serial dilution was then performed to create concentrations that ranged from 13.3 μM to 2.0 nM. The 80% volume concentrated media rediluted to 100% volume with pure sterile water with no drug added was used as the control for each condition. The incubation media in each well was then

replaced with the above prepared solutions causing minimal disturbance to the cells. The cells were allowed to incubate at 37°C for 72 h.

At 72 hours, the In Vitro Toxicology Assay Kit (TOX2) from Sigma Aldrich was used to perform an XTT cell viability assay. Phenol red free DMEM media containing 10% Fetal Bovine Serum and penicillin-streptomycin from Gibco was used for the XTT assay to prevent phenol red interference with the absorption measurements. After 30 min of incubation time, the absorbance of each well was measured using a Tecan Infinite M200 plate reader (San Jose, CA, USA). The collected absorbance values were used to create percent viability vs. dose curves with the PRISM 4.0 program from GraphPad Software Inc. (La Jolla, CA, USA) using the sigmoidal dose-response (variable slope) curve fit. IC_{50} values were then determined from the fitted curves. The statistical analysis was performed using MATLAB R2015a software.

3. Results and Discussion

3.1 Nanoparticle Preparation and Characterization

The prodrug compound, called Doxorubicin-Photocleavable Biotin (DOX-PCB), was formed by blocking the free amine located on the sugar moiety of DOX with a nitrophenyl group conjugated to a short polyethylene glycol linker and terminated with a biotin (PCB) as seen in Figure 2A. The structure of DOX-PCB has been characterized using high resolution mass spectrometry, HPLC/mass spectrometry, and absorption spectral analysis.(12) Three dimensional modeling of the molecular conformation of DOX-PCB in water using ChemDraw is shown in Figure 2B. This hairpin shape results from the hydrophobic aglycone structure of DOX interacting with the hydrophobic nitrophenyl group. This gives the molecule a hydrophobic head and a hydrophilic tail consisting of the PEG linker and biotin (Figure 2C). We hypothesized that this dual hydrophobic/hydrophilic structure would allow the prodrug molecules to self-assemble into nanoparticles upon injection into aqueous solution using a nanoprecipitation process.

As described in the methods section, we successfully used a single-step nanoprecipitation process to fabricate the first nanoparticles made entirely from light-activatable prodrug (Figure 2D and E). The self-assembly fabrication method of DOX-PCB nanoparticles is relatively simple, giving it strong potential for future scale-up. Size results obtained using Dynamic Light Scattering (DLS) showed that the DOX-PCB nanoparticles had a unimodal size distribution with an average diameter of 102 ± 2 nm as shown in Table 1. Size results obtained from Nanoparticle Tracking Analysis (NTA, Table 1) confirmed the nanoparticle size at approximately 100 nm in diameter. Zeta potential was measured at −42 ± 4 mV, which supports that the nanoparticles have sufficient repulsive interactions to be stably monodispersed in solution.

Scanning electron microscope images of the DOX-PCB nanoparticles are shown in Figure 2E. The particles are spherical in shape with a size range that appears slightly smaller than the results obtained by DLS and NTA, which may be an effect of the nanoparticles dehydrating during the drying preparation used for SEM.

The surface coating of the nanoparticles was studied by observing their interaction with streptavidin-coated Sepharose microbeads. If the hydrophilic biotin-terminated PEG tail of the DOX-PCB molecule formed a coating on the surface of the nanoparticles, then we would expect the biotin to strongly attach to the avidin on the coated microbeads. Since the DOX-PCB nanoparticles are inherently fluorescent we could monitor this binding interaction by fluorescence imaging. In Figure 3A, there is a strong fluorescence signal on the avidin coated microbeads arising from the DOX-PCB nanoparticles binding to the surface. Bare Sepharose beads showed no fluorescence signal indicating that there was no nonspecific nanoparticle binding (Figure 3B).

The results from Figure 2E and Figure 3 indicate that when nanoprecipitated, the prodrug molecules form a spherical cluster comprising the core of the nanoparticle while the molecules at the surface point their hydrophilic tails into the water as shown in Figure 2D.

The DOX-PCB nanoparticles were able to be concentrated to at least 0.22 mg/ml without aggregation. This also supports that the prodrug molecules on the outer layer of the nanoparticle oriented themselves such that the PEG chain interfaced with the water and prevented hydrophobic interactions between particles and subsequent aggregation. The particles maintained a stable size in water at 4°C for over 6 months.

These nanoparticles were formed using only the light-activatable prodrug molecules themselves without the need for any support scaffold. This utilized the entire volume of the nanoparticle to carry prodrug thereby maximizing the payload capacity. This is different from most other nanoparticle designs that require a scaffolding or structural barrier to contain the drug payload. These structural components take up valuable volume inside the nanoparticle which reduces the amount of payload that can be loaded.

The DOX-PCB nanoparticles have a ~ 99% loading efficiency of the prodrug as determined by high pressure liquid chromatography showing very low quantities (< 2%) of DOX-PCB left in the supernatant after the nanoparticles were removed from the synthesis solution through filtration.

3.2 Light Activation and DOX Release

Release of the active DOX from the DOX-PCB nanoparticles was studied by exposing samples of the particles to constant levels of 365 nm light for periods of time that ranged from 5 to 60 min. Significantly increasing amounts of pure DOX were released from the nanoparticles upon increasing 365 nm light exposure as shown in Figure 4. The amounts of released DOX at t=0, 5, and 60 min were found to be significantly different from one another ($P \leq 0.05$) in direct comparisons using a two-sample t-test (two-sided) performed at a 5% significance level. This shows clear increases in DOX quantity over time. A high rate of release was observed within the first 5 min of light exposure followed by a slower rate of release. This second release rate was observed to be linear with the 365 nm light exposure time ($R^2 = .97$) (Figure 4). This indicates that an increase in the amount of light exposure results in a greater amount of DOX release.

3.3 Cellular Localization

The localization of free DOX and the DOX-PCB nanoparticles in the PTK2 kidney epithelial cell line is shown in Figure 5. Both DOX and DOX-PCB are inherently fluorescent allowing them to be tracked within a cell. The PTK2 cells were chosen due to their unique tendency to remain flat during mitosis improving the ability to image the nuclear DNA and determine cellular localization. One of the known modes of therapeutic action of pure DOX is by DNA intercalation,(30) and through interactions with DNA polymerase I and topoisomerase II.(31) Free DOX is seen to strongly associate with the cell nuclei as shown in panel 5B. Prior to 365 nm light exposure (Figure 5D), the DOX-PCB in the nanoparticles can be seen in the cell cytoplasm possibly binding to the Golgi apparatus or the endoplasmic reticulum, but not associating with the cell nuclei which remain dark. After exposure to the 365 nm light, the nuclei of the cells show increased fluorescence (Figure 5F) indicating that the DOX released from DOX-PCB was associating with the nucleus as therapeutically expected.

3.4 Cytotoxicity of the DOX-PCB Nanoparticles

Figure 6 shows A549 human lung cancer cell cytotoxicity data under three different experimental conditions including incubation with the DOX-PCB nanoparticles before light exposure, incubation with an equal dose of free DOX, and incubation with the DOX-PCB nanoparticles after light exposure. A549 cancer cells were chosen due to their known sensitivity to DOX. Before exposure to light, the DOX-PCB nanoparticles displayed a significant reduction in toxicity and a 30-fold reduction in IC_{50} concentration when compared to the same dose of free DOX (IC_{50} value of 4.37 μM for DOX-PCB NP and 0.14 μM for DOX). The observed lack of interactions between the DOX-PCB prodrug and the cellular DNA shown in Figure 5D could contribute to this reduction in toxicity.

As shown in Figure 4, pure DOX was released from the nanoparticles upon exposure to 60 min of 365 nm light (2.3 mW/cm^2). This free DOX significantly increased the toxicity of the entire sample and reduced the IC_{50} value to 1.58 μM. The DNA intercalation of the released DOX shown in Figure 5F would have contributed to the photoactivated sample's observed increase in cellular toxicity.

The number of DOX-PCB prodrug molecules that convert to pure DOX can be increased by increasing the dose of light through the use of higher power LED light sources or by increasing the exposure time as shown in Figure 4. The release of more DOX would increase the cellular toxicity of the DOX-PCB nanoparticle sample and would result in a further reduction of the IC_{50}.

The unique light-activatable properties of the DOX-PCB nanoparticles make them promising as a means to locally control the production of pure DOX within tumor tissue while sparing healthy tissue throughout the body from toxic levels of DOX exposure. The size and surface characteristics of the DOX-PCB nanoparticles make them likely to accumulate in tumor tissue and also in specific sites of healthy tissue including the bone marrow and the hands and feet in a similar manner observed with Doxil®. However, the demonstrated reduction in toxicity of the DOX-PCB prodrug payload would make this unavoidable accumulation of the prodrug less toxic to the healthy tissue compared to an equivalent accumulation of DOX.

This could result in reduced skin ulcerations in the hands and feet as well as reduced bone marrow toxicity which would significantly reduce dose-limiting side effects and improve patient quality of life during treatment.

Along with this reduction in off-target toxicity comes the ability to therapeutically treat the tumor tissue because pure DOX would only be released from the particles that have accumulated inside the 365 nm light-exposed tumor tissue (Figure 1). The successful delivery of the light to tumor tissue has already been demonstrated in mouse models(13) and can be developed for human use as implantable LED systems allowing for long exposure times that can stretch into multiple hours or even days.

A unique potential of this technique is that by adjusting the intensity or delivery schedule of the 365 nm light, the DOX release rate could be tailored to make DOX bioavailable from the accumulated particles at a rate that results in the greatest tumor response.

The overall reduction in the toxicity of the DOX-PCB nanoparticles also opens up the possibility of giving a higher dose of these nanoparticles to patients than what can be achieved using Doxil®. This might result in overall higher doses of pure DOX accumulation in tumor tissue after light activation.

The water solubility of DOX-PCB was greatly improved by the nanoparticle formulation. Free DOX-PCB molecules have very low water solubility and could not be detected in water using mass spectrometry analysis. However, with the nanoparticle formulation we were able to achieve a concentration of 200 μM DOX-PCB in water. The increased solubility is likely due to the hydrophilic surface of the nanoparticle that is formed by the hydrophilic tails of the DOX-PCB molecules located at the particle surface as demonstrated in Figure 3.

The use of high concentrations of Captisol® cyclodextrin can also greatly enhance the water solubility of DOX-PCB molecules as has been used previously for *in-vivo* administration. (13) However, the new DOX-PCB nanoparticle formulation presented here has several advantages over the cyclodextrin formulation.

The cyclodextrin keeps the DOX-PCB soluble in saline only when the cyclodextrin is at high concentrations before injection but not when diluted in blood. Thus the circulation half-life and biodistribution of DOX-PCB are subject to the properties of the DOX-PCB molecule itself and not associated with the cyclodextrin carrier. Changing the circulation properties of the free DOX-PCB molecules would require chemical modifications of the DOX-PCB molecules themselves, which could have negative impacts on their desirable properties such as the hairpin conformation and light activation.

The nanoparticle formulation maintains the solubility of DOX-PCB even when diluted into cell culture media. The biodistribution and circulation half-life of DOX-PCB in the nanoparticle formulation will likely be heavily dependent on the nature of the nanoparticle as discussed in the introduction. The resulting changes to biodistribution and circulation half-life would occur without having to make any chemical changes to the DOX-PCB molecule. In the future, further changes to the biodistribution and circulation properties of the nanoparticles can be made by adding surface coatings to the nanoparticles also without

changing the DOX-PCB molecular structure. The nanoparticle formulation is also less viscous than the cyclodextrin formulation which makes it easier for intravascular injection.

4. Conclusions

The proof-of-concept work described here demonstrates the ability to create self-assembled nanoparticles entirely from light-activated prodrug molecules. These nanoparticles have an average diameter of about 100 nm and feature a PEG coating that interfaces between the core of the particle and the surrounding water. These particles were shown to be significantly less toxic to A549 human lung cancer cells compared to pure DOX with a 30 times reduction in IC_{50}. The DOX-PCB prodrug nanoparticles did not show any evidence of interaction with cellular DNA which likely contributed to the reduction in toxicity. Upon exposure to 365 nm light, pure DOX was released from the nanoparticles in significantly increasing amounts with a linear dose response. The released DOX was shown to associate with the cellular DNA significantly increasing the toxicity of the sample. The stability and size properties of the DOX-PCB nanoparticles along with the ability to release DOX when exposed to 365 nm light make these particles promising for future *in-vivo* studies to reduce active DOX concentrations in healthy tissues that actively and passively accumulate nanoparticles while simultaneously delivering a therapeutic dose of DOX to tumor tissue.

Acknowledgements

Support was provided by Grant Numbers T32 CA121938, R25 CA153915, and 5 U54 CA119335 from the National Cancer Institute. The content is solely the responsibility of the authors and does not necessarily represent the official views of the National Cancer Institute or the National Institutes of Health. The authors also wish to thank Dr. Yongxuan Su and the Molecular Mass Spectrometry Facility at the University of California San Diego Department of Chemistry and Biochemistry for their work with the mass spectrometry analysis. The authors also wish to thank Linda Shi and Michelle Duquette-Huber for their assistance with the PTK2 cell data collection.

Abbreviations

DLS	Dynamic light scattering
DMEM	Dulbecco’s Modified Eagle Medium
DMSO	Dimethyl sulfoxide
DOX	Doxorubicin
DOX-PCB	Doxorubicin-Photocleavable Biotin
DPBS	Dulbecco’s phosphate buffered saline
EDTA	Ethylenediaminetetraacetic acid
ESI	Electrospray ionization
FBS	Fetal bovine serum
HPLC	High pressure liquid chromatography
LC	Liquid chromatography

LED	Light emitting diode
MS	Mass spectrometry
NP	Nanoparticles
NTA	Nanoparticle Tracking Analysis
PCB	Photocleavable biotin
PEG	Polyethylene glycol
RES	Reticulo-endothelial system
SEM	Scanning electron microscopy
SRM	Selected reaction monitoring

References

1. Gabizon AA. Pegylated Liposomal Doxorubicin: Metamorphosis of an Old Drug into a New Form of Chemotherapy. Cancer Investigation 2001;19(4):424–436. [PubMed: 11405181]
2. Pawan K Singal NI Doxorubicin-Induced Cardiomyopathy. The New England Journal of Medicine 1998;339(13):900–905. [PubMed: 9744975]
3. Olson RDMP. Doxorubicin cardiotoxicity: analysis of prevailing hypotheses. FASEB J 1990;4(13): 3076–3086. [PubMed: 2210154]
4. Minotti PM Giorgio, Salvatorelli Emanuela, Cairo Gaetano, Gianni Luca. Anthracyclines: Molecular Advances and Pharmacologic Developments in Antitumor Activity and Cardiotoxicity. Pharmacol Rev 2004;56:185–229. [PubMed: 15169927]
5. Charrois G, Allen T. Multiple Injections of Pegylated Liposomal Doxorubicin: Pharmacokinetics and Therapeutic Activity. J Pharmacol Exp Ther 2003 306(3):1058–1067. [PubMed: 12808004]
6. Judson I, Radford JA, Harris M, Blay JY, Van Hoesel Q, Le Cesne A, Van Oosterom AT, Clemons MJ, Kamby C, Hermans C. Randomised phase II trial of pegylated liposomal doxorubicin (DOXIL®/CAELYX®) versus doxorubicin in the treatment of advanced or metastatic soft tissue sarcoma: a study by the EORTC Soft Tissue and Bone Sarcoma Group. European Journal of Cancer 2001;37(7):870–877. [PubMed: 11313175]
7. Gabizon A, Shmeeda H, Barenholz Y. Pharmacokinetics of pegylated liposomal doxorubicin. Clinical pharmacokinetics 2003;42(5):419–436. [PubMed: 12739982]
8. Owens DE III, Peppas NA. Opsonization, biodistribution, and pharmacokinetics of polymeric nanoparticles. International journal of pharmaceutics 2006;307(1):93–102. [PubMed: 16303268]
9. Gaumet M, Vargas A, Gurny R, Delie F. Nanoparticles for drug delivery: the need for precision in reporting particle size parameters. European journal of pharmaceutics and biopharmaceutics 2008;69(1):1–9. [PubMed: 17826969]
10. Gabizon A, Catane R, Uziely B, Kaufman B, Safra T, Cohen R, Martin F, Huang A, Barenholz Y. Prolonged Circulation Time and Enhanced Accumulation in Malignant Exudates of Doxorubicin Encapsulated in Polyethylene-glycol Coated Liposomes. Cancer Research 1994;154:987–992.
11. Amit B, Zehavi U, Patchornik A. Photosensitive Protecting Groups of Amino Sugars and Their Use in Glycoside Synthesis. 2-Nitrobenzyloxycarbonylamino and 6-Nitroveratryloxycarbonylamino derivatives. J Org Chem 1974;39:192–196.
12. Ibsen S, Zahavy E, Wrasidlo W, Berns M, Chan M, Esener S. A Novel Doxorubicin Prodrug with Controllable Photolysis Activation for Cancer Chemotherapy. Pharmaceutical Research 2010;27(9):1848–1860. [PubMed: 20596761]
13. Ibsen S, Zahavy E, Wrasidlo W, Hayashi T, Norton J, Su Y, Adams S, Esener S. Localized In-Vivo Activation of a Photoactivatable Doxorubicin Prodrug in Deep Tumor Tissue. Photochemistry and photobiology 2013;89:698–708. [PubMed: 23311544]

14. Tietze LF, Mollers Thomas, Fischer Roland, Glusenkamp Karl-Heinz, Rajewsky Manfred F., and Jahde Eckhard. Proton-mediated Liberation of Aldophosphamide from a Nontoxic Prodrug: A Strategy for Tumor-selective Activation of Cytocidal Drugs. Cancer Research 1989;49:4179–4184. [PubMed: 2743306]
15. Brown WRW J.Martin. Exploiting Tumor Hypoxia in Cancer Treatment Nature Reviews Cancer 2004;4:437–447.
16. Breistol HRHK, Berger DP, Langdon SP, Fiebig HH, and Fodstad O. The Antitumour Activity of the Prodrug N-l-leucyl-doxorubicin and its Parent Compound Doxorubicin in Human Tumour Xenografts. European Journal of Cancer 1998;34(10):1602–1606. [PubMed: 9893636]
17. Gopin A, Ebner S, Attali B, Shabat D. Enzymatic Activation of second-generation dendritic prodrugs: Conjugation of self-immolative dendrimers with PEG via click chemistry. Bioconjugate Chem 2006;17:1432–1440.
18. Shamis M, Lode HN, Shabat D. Bioactivation of self-immolative dendritic prodrugs by catalytic antibody 38C2. JACS 2004;126:1726–1731.
19. Park J, Hong K, Kirpotin D, Colbern G, Shalaby R, Baselga J, Shao Y, Nielsen U, Marks J, Moore D, Papahadjopoulos D, Benz C. Anti-HER2 Immunoliposomes: Enhanced Efficacy Attributable to Targeted Delivery. Clinical Cancer Research 2002;8:1172–1181.
20. Vaupel P, Kallinowski F, Okunieff P,. Blood Flow, Oxygen and Nutrient Supply, and Metabolic Microenvironment of Human Tumors: A Review. Cancer Research 1989;49:6449–6465. [PubMed: 2684393]
21. Ni T, Baudisch P. Disappearing mobile devices. In.Proceedings of the 22nd annual ACM symposium on User interface software and technology Victoria, British Columbia, Canada: Association for Computing Machinery; 2009 p. 101–110.
22. Miwa M, Ura M, Nishida M, Sawada N, Ishikawa T, Mori K, Shimma N, Umeda I, Ishitsuka H. Design of a novel oral fluoropyrimidine carbamate, capecitabine, which generates 5-fluorouracil selectively in tumours by enzymes concentrated in human liver and cancer tissue. European Journal of Cancer 1998;34(8):1274–1281 [PubMed: 9849491]
23. Yang EJC Yuanlong, Koutcher Jason A., Alfano RR. UV Reflectance Spectroscopy Probes DNA and Protein Changes in Human Breast Tissues. Journal of Clinical Laser Medicine & Surgery 2001;19(1):35–39. [PubMed: 11547817]
24. Sutherland J, Griffin K. Absorption Spectrum of DNA for Wavelengths Greater than 300 nm. Radiation Research 1981;86(3):399–410. [PubMed: 6264537]
25. Elisseeff KAJ, Sims D, McIntosh W, Randolph M, and Langer R. Transdermal photopolymerization for minimally invasive implantation. Proc Natl Acad Sci 1999;96:3104–3107. [PubMed: 10077644]
26. Miele E, Spinelli GP, Miele E, Tomao F, Tomao S. Albumin-bound formulation of paclitaxel (Abraxane® ABI-007) in the treatment of breast cancer. International Journal of Nanomedicine 2009;4:99–105. [PubMed: 19516888]
27. Gabizon A, Tzemach D, Mak L, Bronstein M, Horowitz AT. Dose dependency of pharmacokinetics and therapeutic efficacy of pegylated liposomal doxorubicin (DOXIL) in murine models. Journal of drug targeting 2002;10(7):539–548. [PubMed: 12683721]
28. Bao A, Goins B, Klipper R, Negrete G, Phillips WT. Direct 99mTc labeling of pegylated liposomal doxorubicin (Doxil) for pharmacokinetic and non-invasive imaging studies. Journal of Pharmacology and Experimental Therapeutics 2004;308(2):419–425. [PubMed: 14610219]
29. Pasqualini R, Arap W, McDonald DM. Probing the structural and molecular diversity of tumor vasculature. Trends in molecular medicine 2002;8(12):563–571. [PubMed: 12470989]
30. Quigley Gary J. Wang Andrew H.-J., Ughetto Giovanni, Van Der Marel Gijs, Van Boom Jacques H., and Rich Alexander. Molecular structure of an anticancer drug-DNA complex: Daunomycin plus d(CpGpTpApCpG). Proc Nati Acad Sc USA 1980;77(12):7204–7208.
31. Gewirtz DA. A Critical Evaluation of the Mechanisms of Action Proposed for the Antitumor Effects of the Anthracycline Antibiotics Adriamycin and Daunorubicin. Biochemical Pharmacology 1999;57:727–741. [PubMed: 10075079]
32. Botvinick EL, Berns MW. Internet based robotic laser scissors and tweezers microscopy. Microscopy research and technique 2005;68(2):65–74. [PubMed: 16228982]

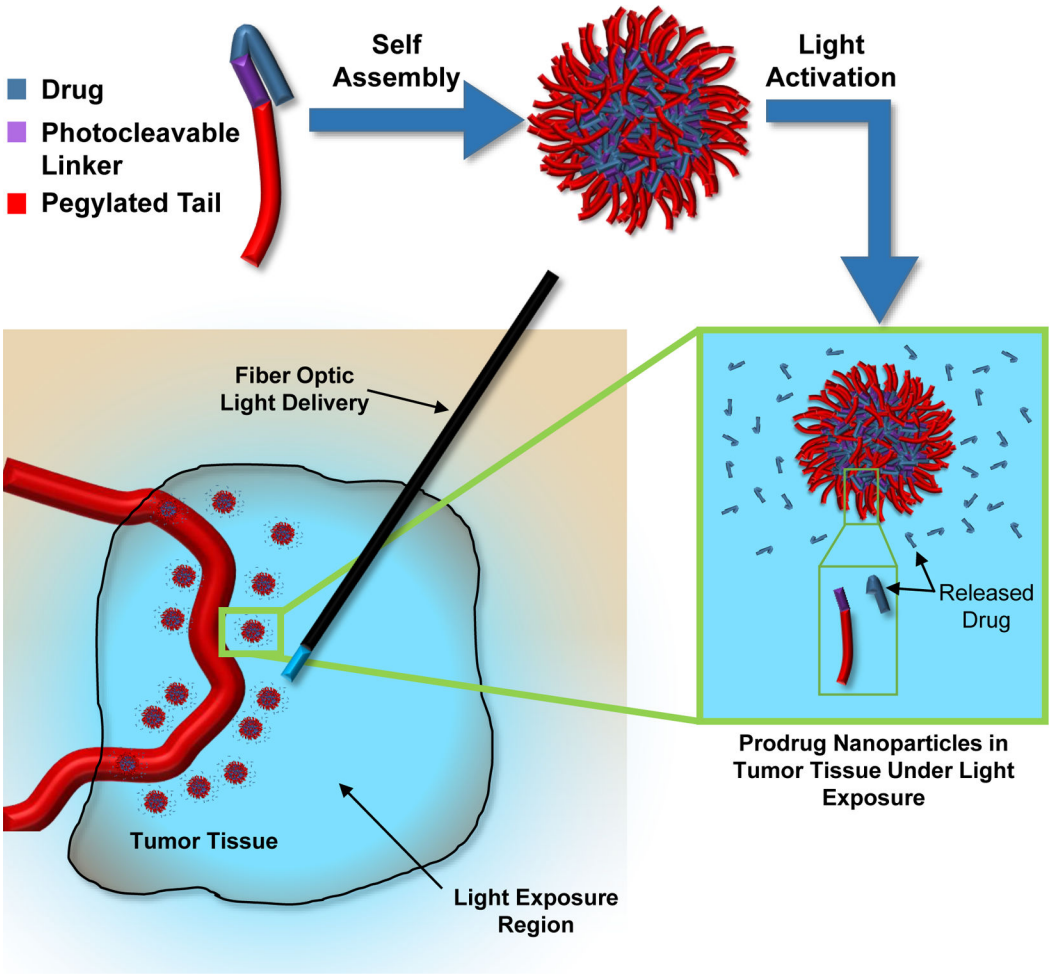

Figure 1.

Schematic representation of the light-activatable prodrug nanoparticle concept. The nanoparticle is self-assembled from light-activatable prodrug molecules. The size of the nanoparticles would allow them to extravasate from circulation through discontinuous endothelium into tumor and healthy tissue. The fiber optic or LED light delivery system exposes just the tumor tissue region where the prodrug is activated and releases highly toxic drug molecules. Nanoparticles that remain in the healthy tissue do not get exposed to the light and remain intact in the low toxicity prodrug form.

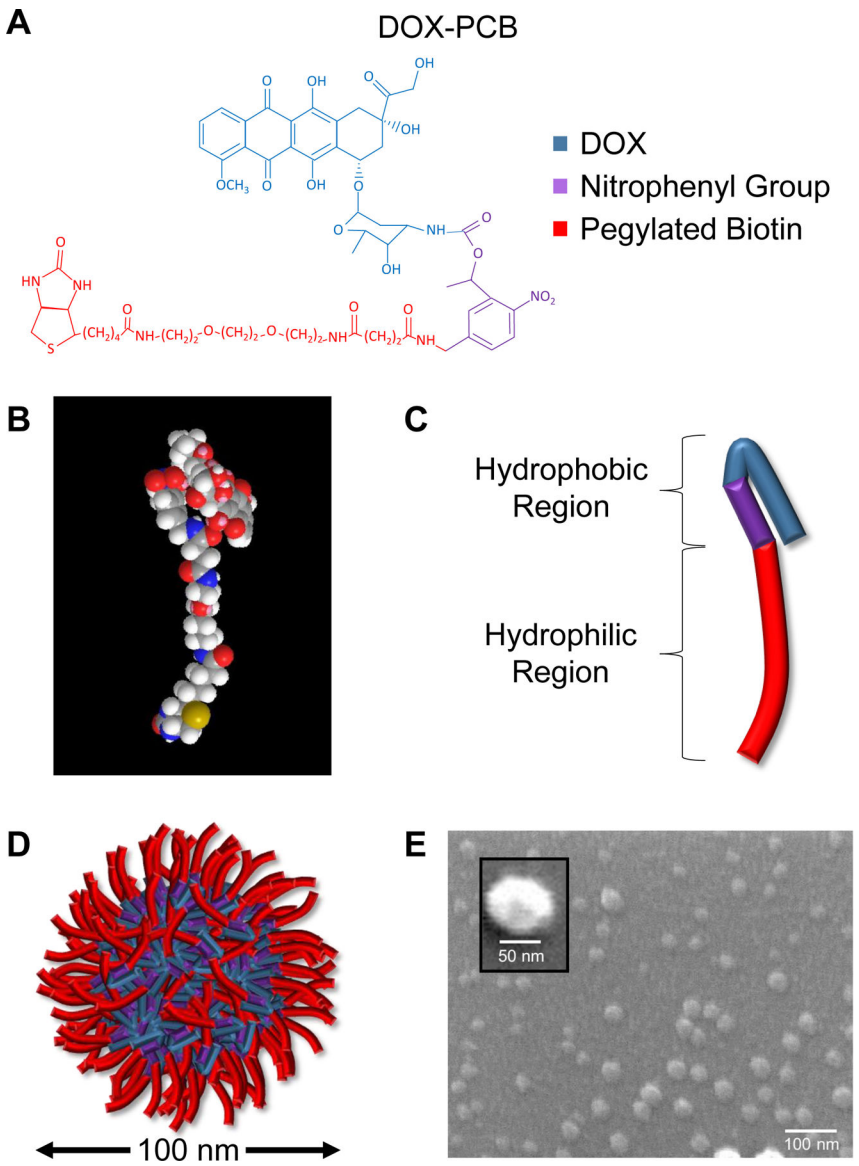

Figure 2.

DOX-PCB nanoparticle structure. **(A)** The prodrug consists of a DOX molecule covalently attached to a photocleavable nitrophenyl compound that has a short polyethylene glycol linker attached to a biotin molecule at the opposite end. **(B)** Three-dimensional conformation of the DOX-PCB prodrug molecule. **(C)** Schematic showing the hydrophobic and hydrophilic regions of the prodrug molecule. The hairpin structural conformation pairs the hydrophobic regions together allowing the hydrophilic tail to extend beyond the bend. **(D)** Schematic of the DOX-PCB nanoparticle. When nanoprecipitated, the molecules cluster to form a core with the biotin tails on the surface. **(E)** Scanning electron microscope image of the DOX-PCB nanoparticles produced by the nanoprecipitation of the DOX-PCB prodrug molecules. The wide field view shows the uniformity of the nanoparticle structures. Inset: SEM image of a single DOX-PCB nanoparticle.

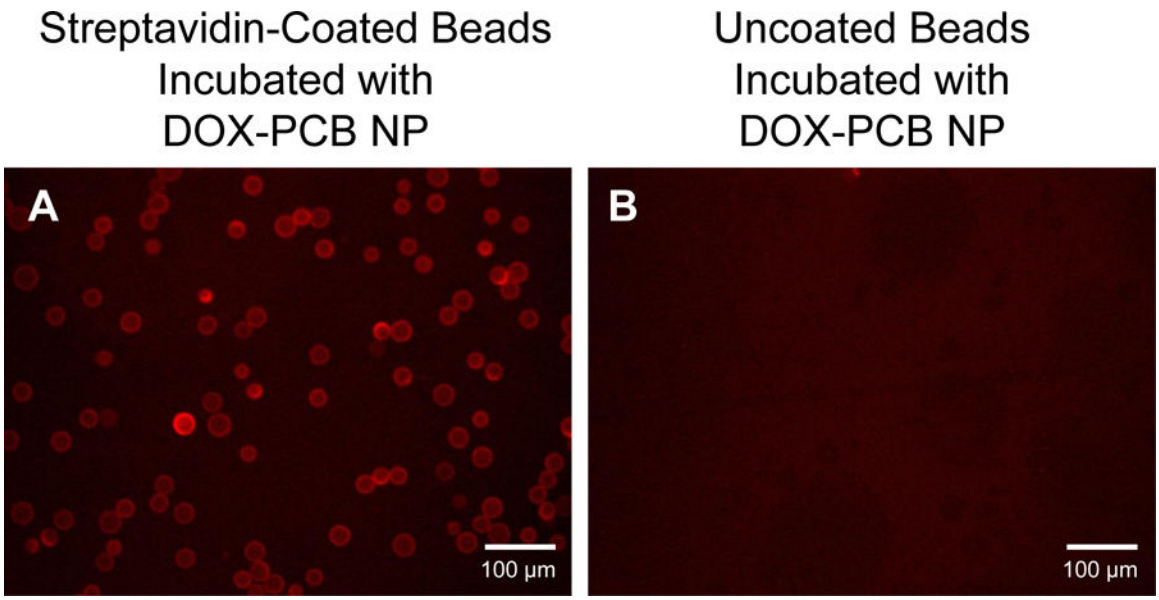

Figure 3.

DOX-PCB nanoparticle surface binding assay. The inherently fluorescent DOX-PCB NPs were incubated with streptavidin-coated Sepharose microbeads and uncoated Sepharose control microbeads. (**A**) The fluorescent DOX-PCB NPs bind to the streptavidin-coated beads outlining their surface. This indicates the presence of the biotin-terminated PEG tail on the surface of the nanoparticles. (**B**) No binding was seen with the uncoated Sepharose control beads.

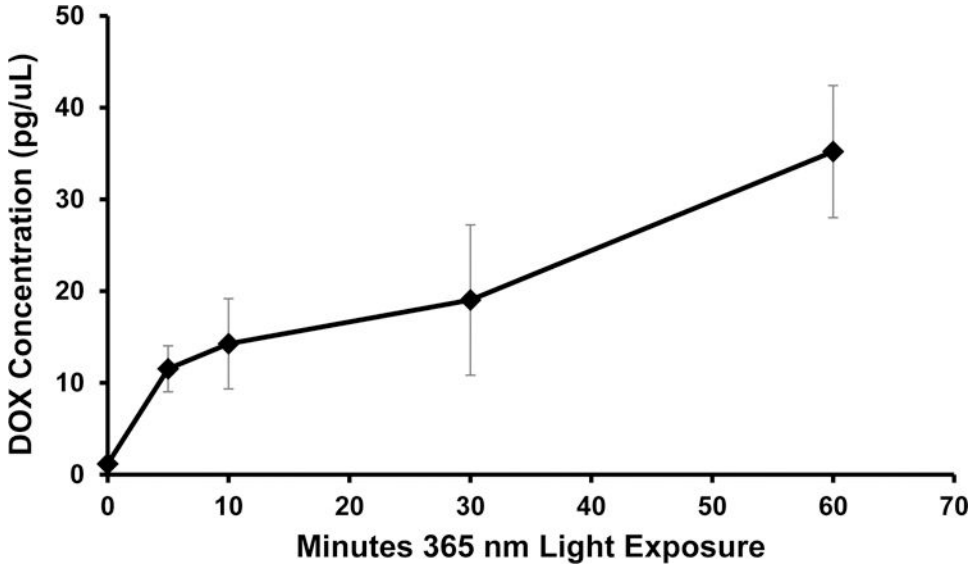

Figure 4.

The concentration of DOX released from the DOX-PCB nanoparticles as a function of 365 nm light exposure. After a higher initial release rate in the first 5 min, the concentration increased in a linear trend with exposure time ($R^2 = 0.97$). Error bars show the standard error of the mean with n=4. These results show that a higher dose of 365 nm light, either in intensity or duration, will result in higher amounts of released DOX.

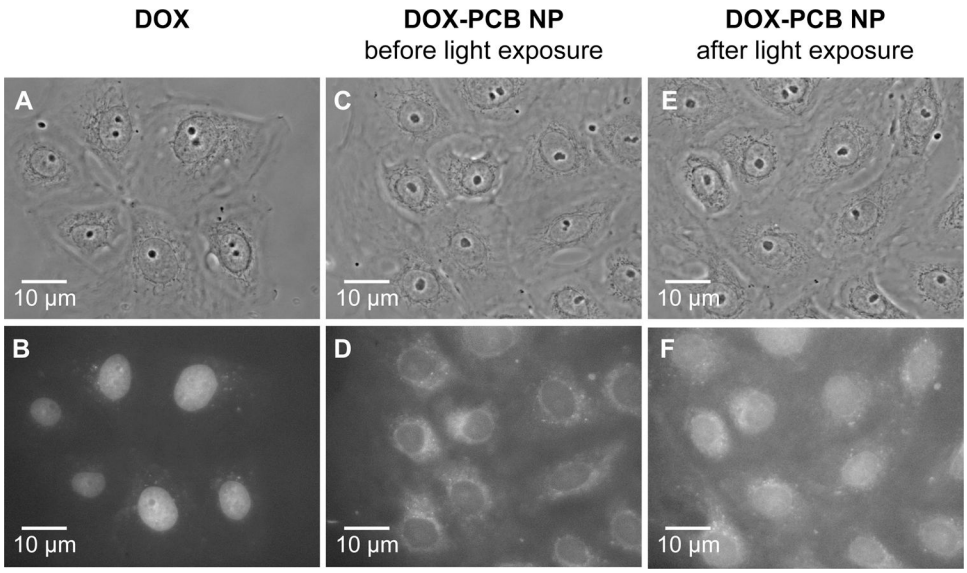

Figure 5.

Light microscopy images of DOX and DOX-PCB nanoparticle localization within live PTK2 kidney epithelial cells. Panels A, C, and E are phase contrast images of the cells and panels B, D, and F are fluorescent images of the same field of view as the panel directly above. Panels C, D, E, and F show the same group of cells before and 1 hour after 365 nm light exposure. **(A, B)** DOX is seen to associate strongly with the cell nuclei. **(C, D)** The cells receiving DOX-PCB nanoparticles showed fluorescence inside the cells but not associated with the nuclei. **(E, F)** After 365 nm light exposure, the nuclei from the same cells shown in C and D show increased fluorescence indicating that free DOX was released from DOX-PCB.

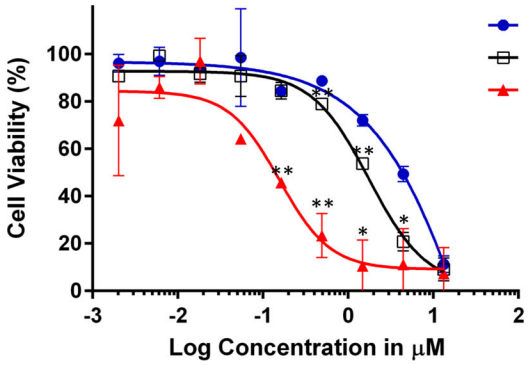

Drug	IC_{50} (μM)
DOX-PCB NP	4.37
DOX-PCB NP (photo-activated 60 min)	1.58
DOX	0.14

Figure 6.

Cytotoxicity results obtained by incubating A549 human lung cancer cells with DOX-PCB nanoparticles, photoactivated DOX-PCB nanoparticles, and free DOX. The graph shows the cell viability curves for the three experimental conditions fitted with a sigmoidal dose-response (variable slope) curve. The resulting IC_{50} values are shown in the table. The DOX-PCB nanoparticles showed a 30-fold higher IC_{50} value than the DOX control. The IC_{50} of the DOX-PCB nanoparticle sample decreased after 60 min of photoactivation. Error bars show the standard deviation. **P ≤ 0.01 and *P ≤ 0.05 by a two-sample t-test (two-sided) performed at the 5% significance level compared to the DOX-PCB NP value at the same time point.

Table 1

Characterization of DOX-PCB nanoparticle size and zeta potential (mean ± standard deviation).

Diameter by DLS (nm)	Polydispersity Index	Diameter by NTA (nm)	Zeta Potential (mV)
102 ± 2	0.120 ± 0.012	96 ± 6	−42 ± 4